

See discussions, stats, and author profiles for this publication at: <https://www.researchgate.net/publication/231681673>

# Role of Betaine as Foam Booster in the Presence of Silicone Oil Drops

ARTICLE *in* LANGMUIR · DECEMBER 1999

Impact Factor: 4.46 · DOI: 10.1021/la990777+

---

CITATIONS

56

---

READS

82

6 AUTHORS, INCLUDING:



**D.N. Ganchev**

14 PUBLICATIONS 319 CITATIONS

SEE PROFILE



**Nikolai D. Denkov**

Sofia University "St. Kliment Ohridski"

151 PUBLICATIONS 5,895 CITATIONS

SEE PROFILE



**Kaoru Tsujii**

Hokkaido University

133 PUBLICATIONS 4,759 CITATIONS

SEE PROFILE

# Role of Betaine as Foam Booster in the Presence of Silicone Oil Drops

Elka S. Basheva,<sup>†</sup> Dragomir Ganchev,<sup>†</sup> Nikolai D. Denkov,<sup>\*,†</sup> Kenichi Kasuga,<sup>‡</sup> Naoki Satoh,<sup>‡</sup> and Kaoru Tsujii<sup>‡,§</sup>

*Laboratory of Thermodynamics and Physicochemical Hydrodynamics, Faculty of Chemistry, Sofia University, 1 James Bourchier Avenue, 1126 Sofia, Bulgaria; Research Laboratories for Hair-Care Products, KAO Corporation, 1–3, Bunka 2-Chome, Sumida-ku, Tokyo, 131-8501 Japan*

*Received June 16, 1999. In Final Form: September 30, 1999*

Betaines (a particular class of amphoteric surfactants) are commonly used as foam boosters in various products to improve their foamability and foam stability. Foaming media often contain dispersed drops of silicone or hydrocarbon oil, which act as foam destruction agents (antifoams). A complementary set of experiments on foams and foam films stabilized by an anionic surfactant, sodium dodecyl-polyoxyethylene-3-sulfate (SDP3S), or by mixtures of SDP3S and Betaine, is performed in the present study to clarify the mechanisms of: (1) foam destruction by silicone oil drops, and (2) foam boosting effect of betaine in the presence of oil. The experiments show that foams stabilized by SDP3S are very stable in the absence of oil, while they are unstable and decay with time in the presence of oil (antifoam effect of the oil). The introduction of 40 molar % betaine in the mixture leads to complete foam stabilization in both cases—with and without oil (foam boosting effect). Notably, the size of the oil droplets has a significant effect on the foam stability—a substantial amount of silicone oil can be introduced without deteriorating the foam stability, if the drop diameter is below ca. 5  $\mu\text{m}$ . Optical observations of the process of foam film thinning show that the oil drops leave the films without destroying them in all of the studied systems (stable and unstable) relatively soon after foam formation—typically, within less than a minute. The foam destruction occurs at a later stage of the foam evolution, when the oil drops are compressed by the walls of the narrowing Plateau channels as a result of liquid drainage from the foam. Surface and interfacial tension measurements show that variations in the values of entry,  $E$ , spreading,  $S$ , and bridging,  $B$ , coefficients cannot be used to explain the observed foam boosting effect of betaine. On the other hand, direct measurements of the critical capillary pressure leading to drop entry demonstrate that the barrier to drop entry is much higher in the presence of betaine. The data unambiguously show that the main role of betaine as a foam booster in the studied systems is to increase the barrier to drop entry, which leads to suppressed activity of the silicone oil as an antifoam. The obtained results provide deeper insight into the foam boosting effect and suggest some clues about the properties which an efficient booster should possess.

## 1. Introduction

Mixtures of amphoteric and anionic surfactants are often used in personal care products to improve their properties.<sup>1</sup> The amphoteric surfactants substantially improve the foamability, foam stability, and rheological behavior of foams, and for this reason are often termed foam boosters in the literature. In addition, the amphoteric decrease the critical micellization concentration of the surfactant mixture, which results in reduced irritation of eyes and skin.<sup>1</sup> Alkylbetaines and alkylamidobetaines, as particular groups of amphoteric surfactants, are typical additives to conditioning shampoos, due to their softening and antistatic effects on hair.<sup>2</sup> Betaines also find industrial application—as softening and wetting agents in textile production, and as emulsifiers in emulsion polymerization, paints, photographic emulsions, and many other systems.<sup>2</sup>

In various cases the foaming medium contains dispersed oil droplets.<sup>3</sup> Thus lanolin or silicone oil are introduced in shampoos to improve their conditioning properties. However, the foamability and foam stability may be deterio-

rated in the presence of oil, which is a very undesirable effect in these systems. The amphoteric surfactants (and betaines, in particular) suppress the so-called antifoam effect of oil droplets, and this is one of the reasons to use them as foam boosters in commercial shampoo formulations. The actual mechanisms of foam destruction by oil additives, and of foam boosting by amphoteric surfactants are still poorly understood, and these are the main subjects of the present study.

The foam destruction by oil substances (hydrocarbons or poly(dimethylsiloxane) oils) has been extensively explored,<sup>3–6</sup> because oil-based antifoams are used in various industries and are important additives to many commercial products, such as detergents, paints, and pharmaceuticals. In these systems the antifoams are introduced to prevent the excessive foam formation. Two mechanisms of foam film destruction by oil additives are usually discussed in the literature: (i) spreading-fluid entrainment<sup>7–10</sup> and (ii) bridging-dewetting.<sup>10–15</sup> According to the spreading mechanism, the oil spreads rapidly

\* Corresponding author. Phone: (+359) 2-962 5310. Fax: (+359) 2-962 5643. E-mail: ND@LTPH.BOL.BG.

<sup>†</sup> Sofia University.

<sup>‡</sup> KAO Corporation.

<sup>§</sup> Current address: Japan Marine Science and Technology Center (JAMSTEC), The DEEPSTAR Group, 2-15 Natsushima-cho, Yokosuka 237-0061, Japan.

(1) *Amphoteric Surfactants*; Lomax, E. G., Ed.; Surfactant Science Series; Marcel Dekker: New York, 1996; Vol. 59.

(2) Domingo, X. In *Amphoteric Surfactants*; Lomax, E. G., Ed.; Surfactant Science Series; Marcel Dekker: New York, 1996; Vol. 59, Chapter 3.

(3) *Defoaming: Theory and Industrial Applications*; Garrett, P. R., Ed. Surfactant Science Series; Marcel Dekker: New York, 1993; Vol. 45.

(4) Aveyard, R.; Binks, B. P.; Fletcher, P. D. I.; Peck, T. G.; Garrett, P. R. *J. Chem. Soc., Faraday Trans.* **1993**, *89*, 4313; Aveyard, R.; Binks, B. P.; Fletcher, P. D. I.; Peck, T. G.; Rutherford, C. E. *Adv. Colloid Interface Sci.* **1994**, *48*, 93.

(5) Pugh, R. J. *Adv. Colloid Interface Sci.* **1996**, *64*, 67.

(6) Wasan, D. T.; Christiano, S. P. In *Handbook of Surface and Colloid Chemistry*; Birdi, K. S., Ed.; CRC Press: Boca Raton, FL, 1997; Chapter 6.

(7) Ewers, W. E.; Sutherland, K. L. *Aust. J. Sci. Res.* **1952**, *5*, 697.

(8) Shearer, L. T.; Akers, W. W. *J. Phys. Chem.* **1958**, *62*, 1264, 1269.

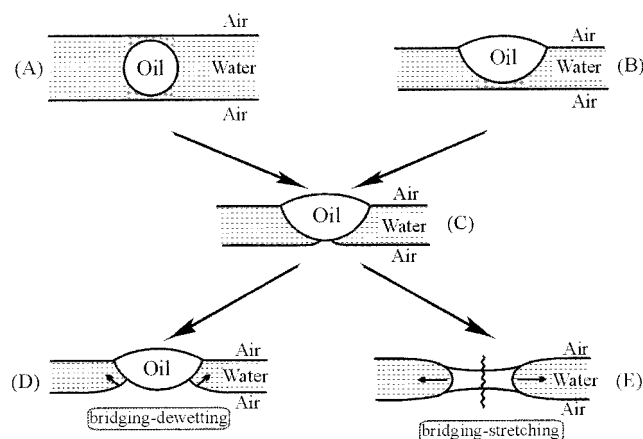


**Figure 1.** Formation of asymmetric oil-water-air films (shaded areas) in some of the possible mechanisms of foam destruction by oil drops or lenses: bridging-dewetting (A-C-D) and (B-C-D); bridging-stretching (A-C-E) and (B-C-E).

over the foam film surface, which leads to a Marangoni-driven flow of liquid in the foam film (fluid entrainment) resulting in a local film thinning and subsequent rupture. For the bridging mechanism an oil drop penetration through both film surfaces is implied, creating an oil bridge between them (Figure 1). The hydrophobic surface of the oil induces a dewetting of the bridge, and a subsequent film rupture. Based on the above concepts the antifoam efficiency is often estimated in terms of the so-called entry coefficient,  $E$ , and spreading coefficient,  $S$ , defined as

$$E = \sigma_{AW} + \sigma_{OW} - \sigma_{OA} \quad (1)$$

$$S = \sigma_{AW} - \sigma_{OW} - \sigma_{OA} \quad (2)$$

where  $\sigma$  are interfacial tensions and the subscripts AW, OW, and OA refer to air-water, oil-water, and oil-air interfaces, respectively. Positive values of  $E$  and  $S$  are considered to correspond to easy entry and spreading of the oil drop, respectively, and to high antifoam efficiency. The critical analysis of the available experimental data made by Garrett<sup>11</sup> has shown that a positive value of  $E$  is a necessary but insufficient condition for having an effective antifoam, which means that other factors might be of critical importance as well. On the other hand, a number of studies<sup>11,13,16-19</sup> have shown that there is no straightforward correlation between the values of  $S$  and the antifoam efficiency.

(9) Prins, A. In *Food Emulsions and Foams*; Dickinson, E., Ed.; Royal Society of Chemistry Special Publication; Royal Society of Chemistry: Letchworth, U.K., 1986; Vol. 58, p 30.

(10) Bergeron, V.; Cooper, P.; Fischer, C.; Giermanska-Kahn, J.; Langevin, D.; Pouchelon, A. *Colloids Surf. A* **1997**, *122*, 103.

(11) Garrett, P. R. In *Defoaming: Theory and Industrial Applications*; Garrett, P. R., Ed.; Surfactant Science Series; Marcel Dekker: New York, 1993; Vol. 45, Chapter 1.

(12) Garrett, P. R.; Moor, P. R. *J. Colloid Interface Sci.* **1993**, *159*, 214.

(13) Garrett, P. R.; Davis, J.; Rendall, H. M. *Colloids Surf. A* **1994**, *85*, 159.

(14) Koczko, K.; Koczko, J. K.; Wasan, D. T. *J. Colloid Interface Sci.* **1994**, *166*, 225.

(15) Aveyard, R.; Cooper, P.; Fletcher, P. D. I.; Rutherford, C. E. *Langmuir* **1993**, *9*, 604.

(16) Kruglyakov, P. M.; Taube, P. R. *Zh. Prikl. Khim.* **1971**, *44*, 129.

(17) Kruglyakov, P. M. In *Thin Liquid Films: Fundamentals and Applications*; Ivanov, I. B., Ed.; Surfactant Science Series; Marcel Dekker: New York, 1988; Vol. 29, Chapter 11.

(18) Kruglyakov, P. M.; Koretskaya, T. A. *Kolloid. Zh.* **1974**, *36*, 682.

(19) Exerowa, D.; Kruglyakov, P. M. *Foams and Foam Films*; Elsevier: Amsterdam, 1998; Chapter 9.

The stability of oil bridges in the bridging-dewetting mechanism can be quantified in terms of another quantity called the bridging coefficient,  $B$ <sup>11,20</sup>

$$B = \sigma_{AW}^2 + \sigma_{OW}^2 - \sigma_{OA}^2 \quad (3)$$

The theoretical analysis predicts that positive values of  $B$  correspond to bridge dewetting and vice versa.

Direct observations of the process of foam film destruction by means of a high speed video camera showed<sup>21</sup> that another mechanism (called bridging-stretching) is responsible for the process of foam destruction by mixed silica-silicone oil antifoams, which are widely used in detergents. This mechanism implies that once an oil bridge is formed in the foam film, this bridge stretches with time, due to uncompensated capillary pressures across the oil-air and oil-water interfaces, and eventually ruptures the film (Figure 1). Formation of such unstable bridges from either initially emulsified antifoam droplets, or from oil lenses floating on one of the film surfaces, bridges the opposing film surface,<sup>10,11,16-19,23-27</sup> see Figure 1. As noted by Kruglyakov<sup>17</sup> and by Kulkarni et al.,<sup>23</sup> this asymmetric film might be stabilized by surface forces (electrostatic, van der Waals, etc.), which suppress the drop entry and impede the antifoam action of oil. Lobo and Wasan<sup>26</sup> suggested the energy of interaction per unit area in the oil-water-air film,  $f$ , while Bergeron et al.<sup>27</sup> proposed the so-called generalized entry coefficient,  $E_g$ , as quantitative measures of the asymmetric film stability. Both quantities are related to the disjoining pressure,  $\Pi_{AS}(h_{AS})$ , which stabilizes the asymmetric film ( $h_{AS}$  is the asymmetric film thickness).

Whatever the mechanism of film destruction is, it includes a stage of formation and rupture of an asymmetric oil-water-air film. This asymmetric film appears when an oil drop approaches the foam film surface, or when an oil lens, floating on one of the film surfaces, bridges the opposing film surface,<sup>10,11,16-19,23-27</sup> see Figure 1. As noted by Kruglyakov<sup>17</sup> and by Kulkarni et al.,<sup>23</sup> this asymmetric film might be stabilized by surface forces (electrostatic, van der Waals, etc.), which suppress the drop entry and impede the antifoam action of oil. Lobo and Wasan<sup>26</sup> suggested the energy of interaction per unit area in the oil-water-air film,  $f$ , while Bergeron et al.<sup>27</sup> proposed the so-called generalized entry coefficient,  $E_g$ , as quantitative measures of the asymmetric film stability. Both quantities are related to the disjoining pressure,  $\Pi_{AS}(h_{AS})$ , which stabilizes the asymmetric film ( $h_{AS}$  is the asymmetric film thickness).

All these studies<sup>10,11,16-19,23-27</sup> stress the significance of the barrier which can prevent particle entry, thus explaining why positive values of the classical entry coefficient,  $E$ , do not necessarily correspond to an easy entry. Indeed, our own experiments unambiguously show that the barrier preventing the drop entry is one of the crucial factors determining the antifoam efficiency. Moreover, one of the main roles of betaine as a foam booster is to increase this barrier.

Another point of discussion in the literature is about the structural element, foam film, or Plateau border, which is actually destroyed by the antifoam drops. The observations described in ref 21 unambiguously demonstrated that the foam destruction by very active mixed silica-silicone oil antifoams occurs through rupture of the foam films, which rapidly thin down to a thickness below 1  $\mu\text{m}$ . On the other hand, Koczko et al.<sup>14</sup> suggested that the antifoam particles (emulsified droplets or lenses) first

(20) Garrett, P. R. *J. Colloid Interface Sci.* **1980**, *76*, 587.

(21) Denkov, N. D.; Cooper, P.; Martin, J.-Y. *Langmuir*, in press.

(22) Denkov, N. D. *Langmuir*, in press.

(23) Kulkarni, R. D.; Goddard, E. D.; Kanner, B. *J. Colloid Interface Sci.* **1977**, *59*, 468.

(24) Wasan, D. T.; Nikolov, A. D.; Huang, D. D. W.; Edwards, D. A. In *Surfactant Based Mobility Control*; Smith, D. H., Ed.; ACS Symposium Series; American Chemical Society: Washington, DC, 1988; Vol. 373, p 136.

(25) Koczko, K.; Lobo, L. A.; Wasan, D. T. *J. Colloid Interface Sci.* **1992**, *150*, 492.

(26) Lobo, L.; Wasan, D. T. *Langmuir* **1993**, *9*, 1668.

(27) Bergeron, V.; Fagan, M. E.; Radke, C. J. *Langmuir* **1993**, *9*, 1704.



escape from the foam films into the neighboring Plateau borders (PB) and get trapped there; only afterward the antifoam particles are compressed within the thinning PBs, which are finally destroyed. Therefore, the results described in the literature suggest that a foam destruction may occur through rupture of either foam films or PBs depending on the particular experimental system; this point deserves further examination.

In the present study we investigate the process of foam destruction by silicone oil for foams stabilized by mixtures of two surfactants: anionic alkyl-polyoxyethylene sulfate as a main foam stabilizer and amphoteric alkylamidobetaine as a foam booster. Experiments with foams and foam films are performed to clarify which structural element is destroyed by the oil drops. The effects of betaine on the entry, spreading, and bridging coefficients, as well as on the barrier to entry of the oil drops, are studied to reveal the physicochemical factor, which is responsible for the foam boosting effect. The results give deeper insight into the studied phenomena and provide some clues about the properties, which an efficient booster should possess.

## 2. Experimental Details

**2.1. Materials.** Sodium dodecyl-polyoxyethylene-3-sulfate (SDP3S) is used as a main surfactant, while lauryl-amide-propylbetaine (hereafter called for brevity betaine) is used as a foam booster in the present study. Both surfactants are of commercial grade (Kao Co., Tokyo, Japan) and are used without further purification. In all experiments the total surfactant concentration is maintained equal to 0.1 M. The commercial surfactant batches contain background electrolytes; SDP3S contains 0.063 g NaCl and 0.024 g Na<sub>2</sub>SO<sub>4</sub> per gram surfactant; betaine contains 0.23 g NaCl per gram surfactant. These electrolytes create an ionic strength of 66 mM in the working solutions of SDP3S and 142 mM in the working betaine solutions. The solutions are prepared with deionized water obtained from a Milli-Q Organex system (Millipore).

Silicone oil SH200 (Kao Co., Tokyo, Japan) of dynamic viscosity 5 mPa·s is used at a typical concentration of 0.1 wt % in the working solutions. Since the solubility of silicone oil in the surfactant solutions is very low, the oil is dispersed in the form of emulsion droplets (see below for the respective procedures).

**2.2. Methods and Procedures.** *2.2.1. Foam Formation and Foam Stability Evaluation.* The Ross–Miles test is used to produce foams and to compare their stability. Briefly, a certain amount of silicone oil (typically 0.1 wt %) is introduced into 300 mL of the surfactant solution. The oil is emulsified by intensive stirring for 20 min on a magnetic stirrer. The emulsion is additionally homogenized by several hand-shakes before placing it into the glass cylinder of the Ross–Miles test. The cylinder has a working volume of 1 dm<sup>3</sup> and diameter of 37 mm. The solution is circulated (pumped) for 20 s, unless another value is specified, at a debit of 125 cm<sup>3</sup>/s through an orifice (7 mm in diameter), which is placed at 23 cm above the level of the liquid. The change of the foam volume with time is monitored for a period of 100 min after liquid circulation ceases. The accuracy in the foam volume determination is  $\pm 2$  mL (determined mainly by the irregular upper boundary of the foam), whereas the reproducibility is typically  $\pm 5$  mL.

For investigating the effect of oil drop size on foam stability, in some of the experiments we dispersed silicone oil in the foaming medium by using a rotor-stator homogenizer Ultra Turrax T25 (Janke & Kunkel GMBH & Co, IKA-Labortechnik). This procedure results in a smaller diameter of the oil drops. The dispersing tool is introduced in a 100 mL laboratory beaker containing 32 mL surfactant solution. The disperse phase (8 mL silicone oil) is added during a period of 10 s while stirring the solution at 8000 rpm. Afterward, the obtained emulsion is additionally homogenized for 5 min at 25 000 rpm. This emulsion is diluted to the working concentration before foam stability experiments. A mild homogenization of the working solution is performed by magnetic stirrer for  $\frac{1}{2}$  h before starting each experiment. For brevity, we call hereafter the emulsions produced

only by magnetic stirrer the coarse emulsions, while the emulsions obtained by rotor-stator homogenizer are termed the fine emulsions.

Most of the experiments are performed with the coarse emulsions, while the fine emulsions are used in one series of experiments for comparison.

*2.2.2. Size Distribution of the Emulsion Droplets.* The size distribution of the emulsion droplets is measured by video-microscopy observations in white transmitted light. A Zeiss Axioplan microscope with objectives 50 $\times$  Epiplan LD, and 100 $\times$  (immersion type) is used. The image is recorded by CCD camera Sony SSC-370CE and VCR Samsung SV-4000W. Then the videotape is processed by homemade image analysis software for determining the drop size distribution. The diameter of several hundred droplets is measured in each sample.

*2.2.3. Surface and Interfacial Tension Measurements.* The surface tension of the surfactant solution is measured by the Wilhelmy plate method on a Kruss K10T digital tensiometer. The tension of the solution surface before and after its contact with silicone oil is determined. After measuring the surface tension of the solution (without oil) 15–30  $\mu$ L of silicone oil is gently deposited on the solution surface away from the Wilhelmy plate. A fast reduction (within 1–2 s) of the surface tension with several mN/m is observed due to spreading of a thin layer of silicone oil over the solution surface. Afterward no detectable change of the surface tension is recorded for a period of 60 min.

The surface tension of the oil is measured by the Du Noy ring technique on a Kruss K10T tensiometer. To check whether the surfactant solution spreads over the oil surface, we employ the following procedure. First, the surface tension of pure silicone oil is measured. Then a drop of the surfactant solution is carefully placed in contact with the oil surface. The drop is kept in contact with the oil surface for at least 2–3 s, and the surface tension of the oil is measured again. In all cases no difference between the measured values of the oil surface tension is detected, indicating that no surfactant spreads on the oil–air interface.

The interfacial tension of the oil–solution interface is measured by the spinning drop method on a Kruss Site 04 tensiometer.

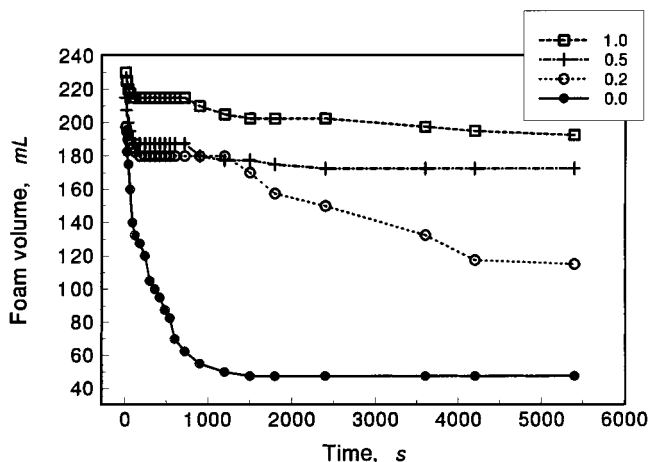
*2.2.4. Stability of Foam Films.* Horizontal foam films of submillimeter size are formed and observed in the so-called Scheludko cell.<sup>28,29</sup> A foam film is formed from a biconcave drop of surfactant solution, placed in a vertical cylindrical glass capillary by sucking out liquid through an orifice in the capillary wall. The amount of liquid in the capillary, and hence the film radius, can be varied by a pressure control system. Special care is taken to suppress water evaporation from the film surfaces. The foam films are observed from above (microscope Zeiss Axioplan, objectives LD Epiplan 10 $\times$  and 50 $\times$ ) in reflected or transmitted white light. The observations in reflected light provide a clear picture of the thin films, while the transmitted light allows one to observe the emulsion droplets in the film or in the meniscus region surrounding it.

*2.2.5. Rate of Thinning and Stability of Vertical Foam Films.* Vertical foam films are formed on a rectangular glass frame (5  $\times$  5 mm). The experimental setup is closed in a transparent glass container, which ensures saturation of the atmosphere around the film with aqueous vapors—the large foam films are extremely vulnerable to rupture if water evaporation is not completely suppressed. The films are observed in monochromatic light ( $\lambda = 550$  nm), which gives one the opportunity to determine the film thickness from the intensity of the light reflected by the film (so-called interferometric method<sup>28–30</sup>). Just after film formation, one sees alternating dark and bright interference stripes moving downward, which indicate that the film thickness is on the order of several hundred nanometers and that the foam film gradually thins with time. As the thickness of the upper part of the film becomes smaller than 100 nm, a very thin (appearing black in reflected light) film region appears there. This thin region expands with time until it occupies the entire film area. Foam film rupture may occur at different stages of the film thinning process depending on the surfactants used and on

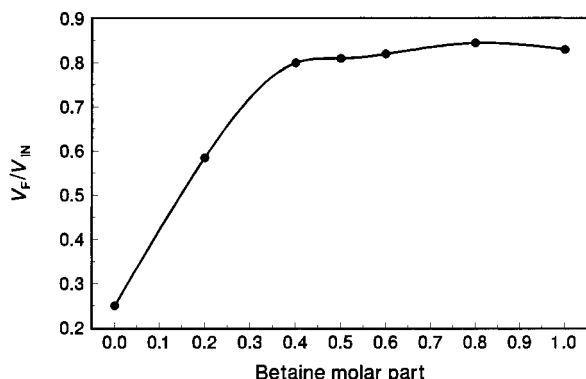
(28) Scheludko, A.; Exerova, D. *Kolloid Z.* **1957**, *155*, 39.

(29) Scheludko, A. *Adv. Colloid Interface Sci.* **1967**, *1*, 391.

(30) Vasicek, A. *Optics of Thin Films*; North-Holland: Amsterdam, 1960.



(A)



(B)

**Figure 2.** (A) Foam volume vs time for different betaine molar fractions in the surfactant mixture: (●) 0, (○) 0.2, (+) 0.5, (□) 1.0; (B) Ratio of the final over initial foam volume vs betaine molar fraction (0.1 M total surfactant concentration; the solution contains 0.1 wt % of silicone oil, coarse emulsion).

the presence of silicone oil. In these experiments we are able to measure the film lifetime, the time needed for the appearance of a black spot inside the film, the velocity of black spot expansion, and the film thickness.

In another set of experiments a different frame is used, similar to that reported previously by Koczko et al.<sup>31</sup> It consists of three vertical legs (1.0 cm long) which meet at the tip of a central capillary at 120°. Three films are simultaneously formed in such a frame with a Plateau border between them, which is not influenced by the solid wall of the glass frame. In this way, one can study the stability of the Plateau borders in the presence of oil drops.

All experiments were performed at an ambient temperature of  $25 \pm 1$  °C.

### 3. Results

This section presents the main experimental observations and their interpretation with respect to the mechanism of foam destruction and the boosting effect of betaine. More general discussion that arranges the results in a unified picture is given in the subsequent Discussion Section.

**3.1. Foam Stability.** *3.1.1. Effect of Betaine on Foam Stability.* The variation of the foam volume with time,  $V(t)$ , is shown in Figure 2A at four different compositions of the surfactant mixture, SDP3S/betaine = 100:0, 80:20, 50:50, and 0:100, in the presence of 0.1 wt % silicone oil (coarse emulsion). In all systems containing betaine, we

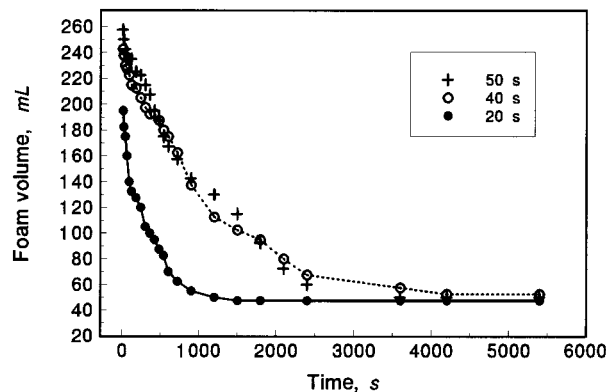


**Figure 3.** Foam volume vs time for different initial circulation (pumping) periods in the Ross–Miles test (0.1 M SDP3S solution containing 0.1 wt % silicone oil, coarse emulsion).

can distinguish three periods of foam evolution. First, one observes an initial period (1–2 min) of intensive liquid drainage from the foam, which leads to reduction of the foam volume of 20–30 mL. The rate of foam drainage rapidly decreases with time and the foam volume remains practically constant during a second period, which takes about 13 min (up to the 15th min after foam formation). The process of bubble coalescence is negligible during the first two periods. Afterward, a slow reduction of the foam volume is observed due to bubble coalescence and foam decay (third period)—this process is pronounced in the system containing the lowest concentration of betaine (final foam volume,  $V_F = 110$  mL), whereas in the other two systems the foam is relatively stable ( $V_F$  above 170 mL).

In the case of SDP3S alone (no betaine) the foam decreases its volume relatively rapidly, and the processes of liquid drainage and foam destruction are not temporarily separated. After approximately 20 min the foam volume in this system levels off at  $V = 48$  mL and no further change is observed during the following 70 min of observation.

The curves shown in Figure 2A demonstrate the foam boosting effect of betaine—a higher concentration of betaine corresponds to a greater final volume of the foam,  $V_F$ . To better illustrate this effect we plot the ratio of the final foam volume,  $V_F$ , over the initial foam volume,  $V_{IN}$ , in Figure 2B, as a function of the betaine molar fraction in the surfactant mixture. As seen from the figure, the foam stability substantially increases with betaine concentration up to the ratio of 60:40 (in the region where SDP3S is in excess), whereas at higher relative concentration of betaine the foam is stable in the studied timescale and no discrimination between the different compositions could be drawn from the results.

Remarkably, we found that the final foam volume in the case of SDP3S (no betaine) slightly depends on the initial foam volume, see Figure 3. Longer pumping periods in the Ross–Miles test, 40 and 50 s, resulted in a higher initial foam column, 243 mL and 258 mL, respectively, against 198 mL for a 20 s pumping period. Nevertheless, the final foam volume was  $50 \pm 2$  mL in all three cases. On the contrary, the final foam volume for stable foams (e.g., pure betaine) depended strongly on the initially produced foam—the bigger the initial foam, the larger the final foam volume. As will be discussed in Section 4, the height of the final foam column can be related to the entry barrier of the oil droplets.

At the end of this subsection it is worth quoting for comparison the initial,  $V_{IN}$ , and the final,  $V_F$ , foam volumes for SDP3S and betaine solutions *in the absence of silicone*

(31) Koczko, K.; Racz, G. *Colloids Surf.* **1987**, *22*, 97.

oil. For pure SDP3S (no betaine)  $V_{IN} = 165$  mL. The liquid drainage leads to reduction of this volume down to 128 mL for about 2 min; afterward no detectable change of the foam volume is observed during the following 88 min. In other words, the foam produced by SDP3S in the absence of silicone oil is *stable*. The foamability of the betaine solution is substantially better,  $V_{IN} = 200$  mL. The foam is also very stable and a final foam volume of 155 mL is established after the period of liquid drainage. Very similar results ( $V_{IN} = 200$  mL,  $V_F = 155$  mL) are obtained with foams produced from an 80:20 mixture of SDP3S and betaine. One can conclude from these observations that the main role of the foam booster in the absence of oil is to increase the initial foam volume (the foam from SDP3S in the absence of silicone oil is stable). In the presence of oil, the booster has an additional very important role, namely, to prevent the process of foam destruction by the oil drops.

**3.1.2. Effect of the Oil Drop Size.** Two series of foam stability experiments were performed with the fine and the coarse emulsions to investigate the effect of the drop size.

The microscope observations showed that the droplets of the fine emulsion had comparatively narrow and unimodal size distribution with a sharp peak at  $3\ \mu\text{m}$ . The average size of the droplets was  $6\ \mu\text{m}$  and the largest observed droplets were of diameter below  $15\ \mu\text{m}$ . Possibly in this emulsion we had small droplets of diameter less than  $1\ \mu\text{m}$  (the optical resolution of the microscope), which were not included in the statistical treatment. In contrast, the coarse emulsion was very polydisperse and the drop size was larger—the main fraction of droplets fell in the range between 4 and  $15\ \mu\text{m}$  in diameter, though a notable fraction of drops was in the range between 15 and  $30\ \mu\text{m}$ . Single droplets of much larger size (around 50 and around  $150\ \mu\text{m}$ ) were observed, while droplets of diameter below  $4\ \mu\text{m}$  were not seen in this sample. The average drop size was  $11\ \mu\text{m}$  by number in the coarse emulsion. These results might be anticipated, keeping in mind that the agitation during the emulsification by means of the magnetic stirrer was relatively mild.

The variation of the foam volume with time for SDP3S at two different concentrations (0.05 and 0.1 wt %) of coarse and fine emulsions is shown in Figure 4. Notably, there is no big difference between the final foam volumes at different concentrations of oil in the case of the coarse emulsion (Figure 4A), while this difference is more than 30 mL in the system containing the fine emulsion (Figure 4B). The same trends were observed at even higher concentration of silicone oil (0.2 wt %), but these results are not shown in the figure to avoid overcrowding.

Similar experiments are performed with an 80:20 mixture of SDP3S/betaine (see Figure 5). Again, the initial and the final foam volumes are larger at the lower concentration of oil, and the foam is more stable in the presence of smaller oil drops (fine emulsion). Moreover, the foam produced from the SDP3S/betaine mixture is extremely stable in the presence of the fine emulsion—after an initial period of liquid drainage, the foam volume remains constant during the whole period of observation and no bubble coalescence takes place (Figure 5B). The final foam volume is above 200 mL in these experiments. The foam produced in the presence of 0.2 wt % of oil in the form of small droplets is also very stable and does not decay during the observation period (not shown in the figure).

These results demonstrate that the size of the silicone droplets is extremely important for foam stability. One can introduce a substantial amount of oil in the foaming

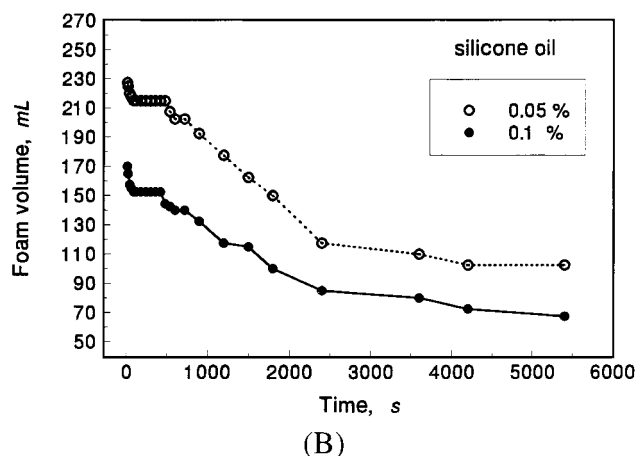
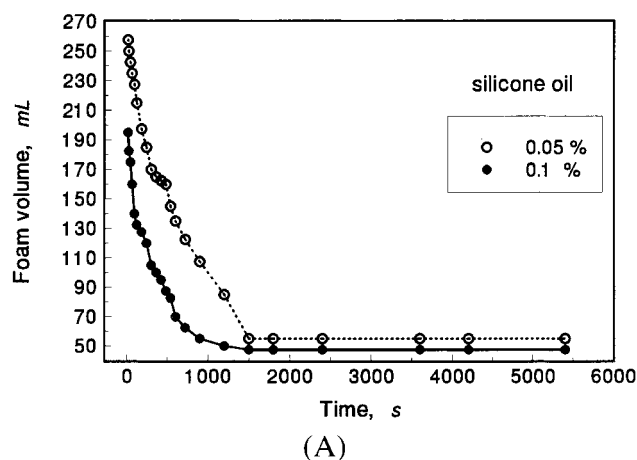


**Figure 4.** Foam volume vs time for different silicone oil concentrations (0.05 or 0.1 wt %) of: (A) coarse emulsion, and (B) fine emulsion (0.1 M SDP3S solution, no betaine).

medium improving the foamability (note that  $V_{IN}$  is larger in the presence of silicone oil) without any deterioration of the foam stability if: (i) the droplets have a diameter of around several micrometers or less, and (ii) there is some fraction of betaine in the surfactant mixture.

**3.2. Entry (E), Spreading (S), and Bridging (B) Coefficients of SDP3S/Betaine Mixtures.** The surface tension of the solutions is measured before and after contact of the surface with a drop of silicone oil. In this way we can calculate the so-called *initial* (before contact of the surface with oil) and *equilibrium* (after saturation of the surface with oil) spreading coefficients.<sup>11</sup> A positive initial spreading coefficient,  $S_{IN}$ , ensures spreading of the silicone oil on the solution surface as a thin layer, typically, several nanometers in thickness. The equilibrium spreading coefficient,  $S_{EQ}$ , could be either negative (which means that oil lenses are in equilibrium with the thin spread layer of oil) or zero (which corresponds to complete spreading of the oil as a duplex film).<sup>32</sup> Similarly, one can define initial and equilibrium entry and bridging coefficients.<sup>11</sup>

The measured values of the interfacial tensions and the calculated values of  $E$ ,  $B$ , and  $S$  coefficients are presented in Table 1. The experimental results can be summarized in the following way. All entering coefficients are positive, i.e., according to the classical theory of antifoaming the entry of the oil drops is thermodynamically favorable. All bridging coefficients are also positive—

(32) Rowlinson, J. S.; Widom, B. *Molecular Theory of Capillarity*; Oxford University Press: Oxford, U.K., 1989; Chapter 8.



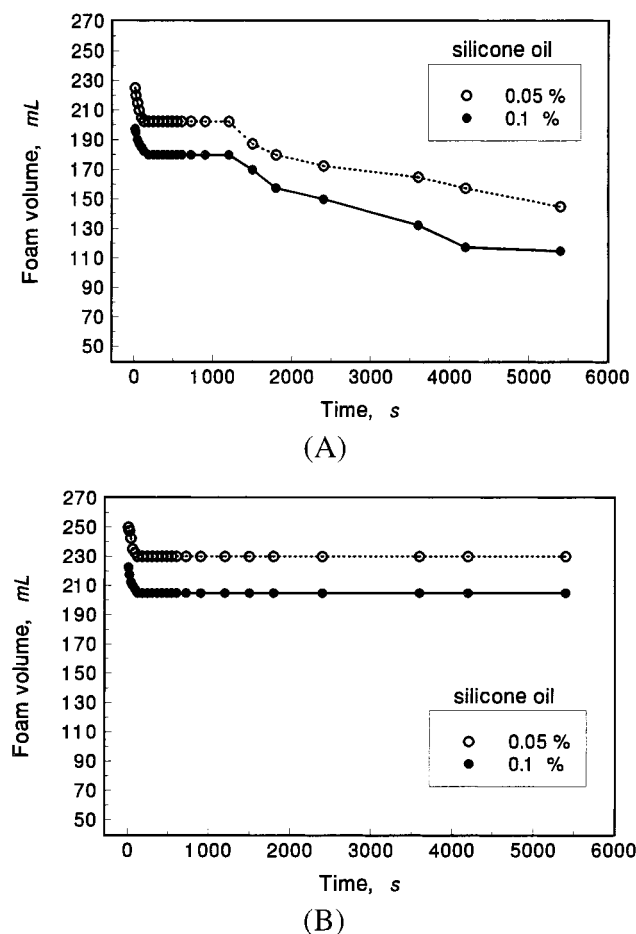


**Figure 5.** Foam volume vs time for different silicone oil concentrations (0.05 or 0.1 wt %) of: (A) coarse emulsion, and (B) fine emulsion (80:20 SDP3S to betaine molar ratio; 0.1 M total concentration).

therefore, oil bridges, once formed in the foam films, should be very unstable. All initial spreading coefficients are also positive, which ensures the spreading of oil in the form of a thin layer. The equilibrium spreading coefficients are negative, which indicates that the oil does not spread as a duplex film; indeed, the oil forms flat lenses on the surface of all solutions after spreading.

In summary, the entry, bridging, and spreading coefficients predict high efficiency of the silicone oil as an antifoam agent in all surfactant systems, which is not observed in the Ross–Miles test. In addition, there is no significant qualitative variation between the coefficients for different solutions that could be used to explain the foam stability in the presence of betaine. For instance,  $E$ ,  $S$ , and  $B$  coefficients for betaine solutions (no SDP3S) are larger than the respective coefficients of the mixture 80:20 SDP3S/betaine. Therefore, according to the classical approach to antifoaming, the foams produced from betaine solutions should be less stable, which is not observed in reality. From these results one can conclude that the relatively weak antifoam activity of the silicone oil in the studied systems (especially in the presence of betaine) is predominantly due to high stability of the asymmetric films, which impedes the entry of the oil drops (see also Section 3.4 below).

**3.3. Stability of Foam Films. 3.3.1. Foam Films in Scheludko Cell.** In these experiments microscope observations of foam films in the presence of emulsion droplets are performed. Therefore, one can perceive whether oil droplets remain in the film sufficiently long to provoke

film rupture. Three series of experiments are performed: (i) without emulsion droplets, (ii) with 0.1 wt % coarse emulsion, and (iii) with 0.1 wt % fine emulsion. In general, the foam films in the Scheludko cell are very stable and the film thinning pattern is practically the same in all these cases. One can discern 5 consecutive stages in the process of foam film thinning (see Figure 6).

**3.3.1.1. Dimple Formation.** A lens shaped formation (called a dimple in the literature<sup>33</sup>), which has a larger thickness in the center, is initially formed upon the mutual approach of two fluid interfaces. Dimples in our system are very unstable—0.1 to 2 s after film formation an asymmetric outflow of liquid from the dimple is observed, and an almost plane-parallel film with several thicker channels is formed (Figure 6A). Some oil droplets are trapped in the dimple when emulsions are studied (coarse or fine), but these droplets leave the film area together with the dimple outflow without film rupture occurring.

**3.3.1.2. Drainage of a Thick Film (Thickness Between 1  $\mu\text{m}$  and 100 nm).** At this stage the film gradually thins down. Several thicker channels are observed in the film area (Figure 6B). Some of the films contain small droplets of diameter below 1  $\mu\text{m}$  (see the arrow in Figure 6B), but these droplets eventually leave the film dragged out by the hydrodynamic flow.

**3.3.1.3. Drainage of a Plane-Parallel Thin Film (Thickness Between 50 and 100 nm).** The hydrodynamic channels gradually disappear and the film becomes rather uniform at a thickness below 100 nm. Even if very small droplets are present in the film at this thickness, they are too small to be seen by direct optical observation.

**3.3.1.4. Film Stratification (Figure 6C,D).** This process of stepwise film thinning occurs in the films of SDP3S at a thickness below 60 nm, due to the so-called colloidal structural forces,<sup>34–39</sup> which appear in films formed from micelle solutions. Theoretical and experimental studies have shown that more or less structured micelle layers are formed in thin films, which give rise to an oscillatory force between the film surfaces. Each stepwise transition corresponds to a reduction of the number of these micelle layers in the film (5 to 4, 4 to 3, etc.). The arrows in Figure 6C depict film areas of different thickness, and the integers indicate the number of micelle layers in the film at the respective film thickness. No oil droplets are present in the foam film at this stage, because the film is too thin.

**3.3.1.5. Black Film.** This is the last stage, when the film is in equilibrium with the surrounding it meniscus region (PB). The film thickness is around 10 nm, so that such films do not contain any oil droplets. Figure 6D represents the moment just before the complete occupation of the film area by the black film.

The first three stages of the film thinning process take a time period of about 1 min. Therefore, the oil drops leave the foam film relatively rapidly (typically, within less than a minute) without destroying it. The fact that the foams in the Ross–Miles test are stable for many minutes means that *the foam destruction by oil droplets occurs in the*

(33) Ivanov, I. B.; Dimitrov, D. S. In *Thin Liquid Films: Fundamentals and Applications*; Ivanov, I. B., Ed.; Surfactant Science Series; Marcel Dekker: New York, 1988; Vol. 29, Chapter 7.

(34) Nikolov, A. D.; Wasan, D. T.; Kralchevsky, P. A.; Ivanov, I. B. *J. Colloid Interface Sci.* **1989**, *133*, 1, 13.

(35) Bergeron, V.; Radke, C. J. *Langmuir* **1992**, *8*, 3020.

(36) Pollard, M. L.; Radke, C. J. *J. Chem. Phys.* **1994**, *101*, 6979.

(37) Chu, X. L.; Nikolov, A. D.; Wasan, D. T. *Langmuir* **1994**, *10*, 4403.

(38) Kralchevsky, P. A.; Denkov, N. D. *Chem. Phys. Lett.* **1995**, *240*, 385.

(39) Kralchevsky, P. A.; Danov, K. D.; Denkov, N. D. In *Handbook of Surface and Colloid Chemistry*; Birdi, K. S., Ed.; CRC Press: New York, 1997; Chapter 11.

**Table 1. Interfacial Tensions<sup>a</sup> with Calculated Entering,  $E$ , Spreading,  $S$ , and Bridging,  $B$ , Coefficients for Silicone Oil in Solutions of SDP3S and Betaine**

betaine molar part	$\sigma_{AW}^{IN}$ mN/m	$\sigma_{AW}^{EQ}$ mN/m	$\sigma_{OW}$ mN/m	$E_{IN}$ mN/m	$E_{EQ}$ mN/m	$S_{IN}$ mN/m	$S_{EQ}$ mN/m	$B_{IN}$ (mN/m) <sup>2</sup>	$B_{EQ}$ (mN/m) <sup>2</sup>
0.0	33.2	25.8	6.8	20.2	12.8	6.6	-0.8	756.4	319.8
0.2	30.4	24.0	5.4	16.0	9.6	5.2	-1.2	561.3	213.1
0.4	28.9	23.1	4.3	13.4	7.6	4.8	-1.0	461.7	160.1
0.5	28.5	23.0	4.2	12.9	7.4	4.5	-1.0	437.8	154.6
0.6	28.2	22.8	4.1	12.5	7.1	4.3	-1.1	420.0	144.6
0.8	28.8	23.4	4.5	13.5	8.1	4.5	-0.9	457.6	175.8
1.0	31.6	26.3	7.2	19.0	13.7	4.6	-0.7	658.4	351.5

<sup>a</sup> In all cases the oil–air tension,  $\sigma_{OA} = 19.8$  mN/m.

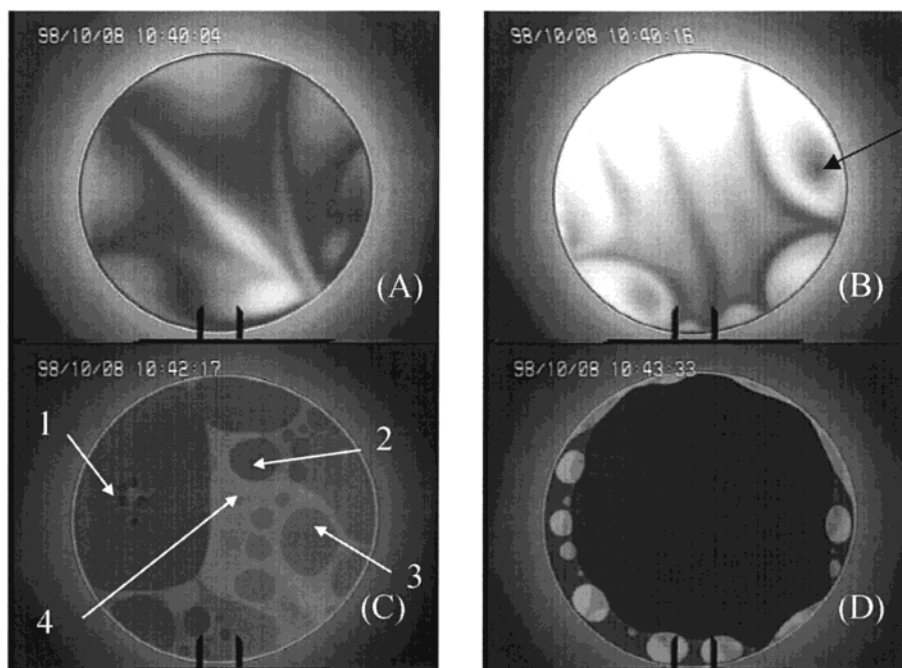


**Figure 6.** Consecutive stages of the process of foam film thinning as observed in reflected light (Scheludko cell): (A) almost planar film containing several thicker channels is formed after the outflow of the dimple from the film; (B) the film gradually thins down; an entrapped oil drop is shown by arrow; (C) a stepwise thinning of the film through formation and expansion of thinner (darker) spots is observed at film thickness below ca. 60 nm; the arrows show film areas containing different numbers of micelle layers, as indicated by the integers; (D) finally, the total film area is occupied by stable black film, which does not contain micelles (0.1 M SDP3S solution, containing 0.1 wt % silicone oil, fine emulsion; the bar is 100  $\mu$ m).

*Plateau channels*, as suggested previously by Koczo et al.<sup>14</sup> (i.e., not in the foam films). Indeed, in a Scheludko cell we frequently observe oil droplets moving in the Plateau border close to film periphery—see Figure 7.

The oil droplets floating around the foam film in the Scheludko cell (Figure 7) do not lead to film rupture, because the Plateau border formed in the cell is very different from the Plateau border in the real foams. In the Scheludko cell the droplets remain more or less free and move around the film contact line (they are not compressed by the air–water interfaces). These drops cannot provoke a rupture of the Plateau border and destruction of the film, because the barrier to drop entry is too high and the drops are arrested within the aqueous phase. In contrast, the Plateau borders in the real foams shrink with time due to gravity driven drainage of liquid from the foam. As a result, the oil drops in foams are compressed and can eventually overcome the barrier to entry. That is why the Scheludko cell is not very suitable for studying the antifoam action of droplets, which destroy the Plateau borders in foams. The film trapping technique discussed below is more pertinent to these systems.

**3.3.2. Experiments with Vertical Foam Films and Plateau Borders (PB).** Four series of experiments are

performed with solutions of SDP3S, betaine, and their 1:1 mixture: (1) experiments with surfactant solutions in the absence of silicone oil; (2) experiments with films obtained from surfactant solutions with a pre-spread layer of silicone oil on the solution surface; (3) experiments in which a layer of silicone oil is spread on the solution surface during the process of film thinning, i.e., after the film has been formed; and (4) experiments with solutions containing emulsified silicone oil (coarse emulsion). Series 1 to 3 are performed with films hung on a rectangular frame, while series 4 is performed with the three-legs frame to observe the effect of oil droplets trapped in the PB.

#### 3.3.2.1. Surfactant Solutions without Silicone Oil.

Figure 8 presents two consecutive stages of the evolution of a vertical foam film obtained from SDP3S solution. In Figure 8A the initial stage of thinning of a relatively thick film (film thickness,  $h > 100$  nm) is illustrated. The horizontal dark and bright stripes in the film correspond to destructive or constructive interference of the light reflected from the two film surfaces.<sup>29,30</sup> These stripes indicate film areas of given thickness, similar to the contours on the topographic map that indicate a given height of the landscape. The stripes move downward, demonstrating the process of gradual film thinning. At



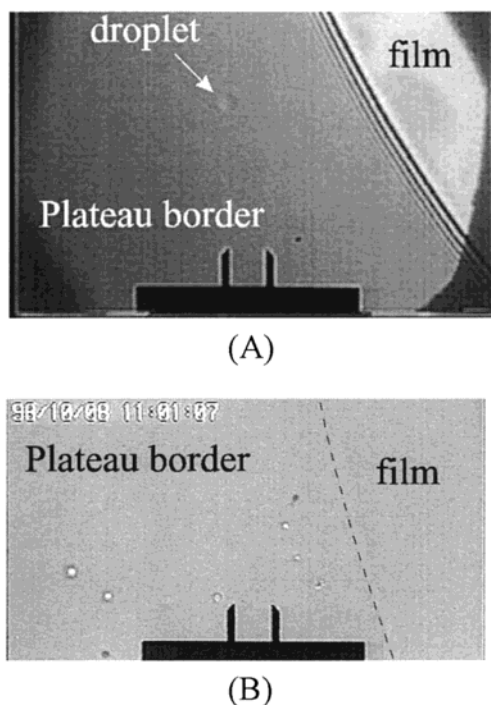


**Figure 7.** The oil drops are expelled from the foam film toward the surrounding Plateau border when the film thickness becomes smaller than the drop diameter: (A) observation in reflected light—one drop is indicated by arrow in vicinity of the film—meniscus boundary; (B) in transmitted light one can see many small drops in the Plateau border (0.1 M SDP3S solution containing 0.1 wt % silicone oil, coarse emulsion).

the film periphery one observes turbulent eddies of uneven thickness which build up the so-called marginal regeneration zone. At a given moment, when the film thickness in the upper part of the film is below 100 nm, a very thin film region (seen as a black spot in reflected light) appears and expands with time—see Figure 8B. After a certain period this thin layer occupies the whole film area. A process of stratification (stepwise thinning) is seen in the films from SDP3S solutions. The films formed from solutions of betaine and its mixture with SDP3S do not exhibit a stratification.

To quantify and to compare the rate of film thinning and the film stability in different systems we measure the following time intervals: (1) the time period for appearance of the black film,  $\tau_{\text{DR}}$  (this period is an indication for the rate of drainage of liquid from the thick film); (2) the time,  $\tau_{\text{E}}$ , for expansion of the black film until it occupies the total film area; and (3) the overall lifetime of the film,  $\tau_{\text{L}}$ . The results for all systems are summarized in Table 2, together with the final film thickness,  $h_{\text{F}}$ , which presents either the equilibrium thickness (if the film is stable) or the thickness at the moment of film rupture (if the film is unstable).

The film thinning in the absence of oil is regular—the film thinning pattern is very reproducible and the films are relatively stable. The latter fact correlates well with the observed high stability of foams in the absence of silicone oil. The drainage time,  $\tau_{\text{DR}}$ , and the time for expansion of the black film,  $\tau_{\text{E}}$ , increase in the order SDP3S, 1:1 mixture of the two surfactants, betaine. Note that the difference between the solutions of SDP3S and the 1:1 mixture of SDP3S/betaine is very small, i.e., one could not explain the boosting effect in the absence of oil with the slower process of film drainage. The final film thickness is practically the same for these two systems. As already mentioned in Section 3.1 above, the main

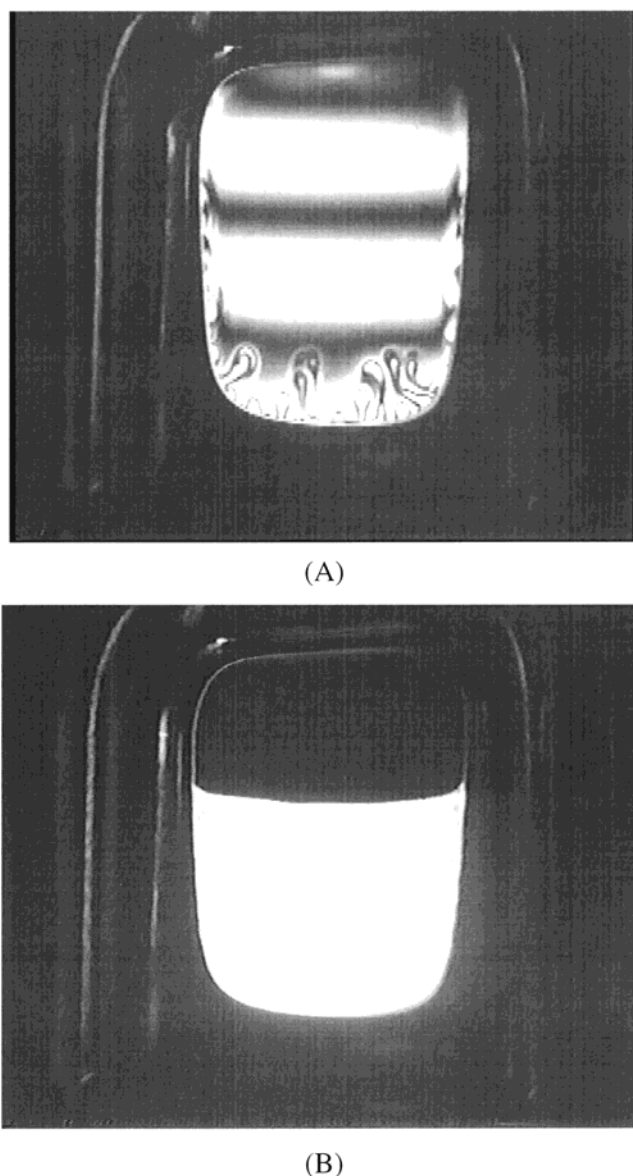


**Figure 8.** Two different stages of thinning of a vertical foam film obtained from 1:1 SDP3S to betaine molar ratio (0.1 M total surfactant concentration, no silicone oil). The horizontal bright and dark interference stripes in (A) indicate regular thinning of a film, whose thickness is about 500 nm; one observes turbulent eddies in the so-called marginal regeneration zone at the film periphery. (B) A very thin black region appears in the upper part of the film at a later stage; this region slowly expands until it occupies the total film area.

**Table 2. Properties of Macroscopic Vertical Foam Films: Film Lifetime ( $\tau_{\text{L}}$ ), Time for Appearance of Black Film ( $\tau_{\text{DR}}$ ), Time for Black Film Expansion ( $\tau_{\text{E}}$ ), and Final Film Thickness ( $h_{\text{F}}$ )**

system	$\tau_{\text{L}}$ [s]	$\tau_{\text{DR}}$ [s]	$\tau_{\text{E}}$ [s]	$h_{\text{F}}$ [nm]
SDP3S	> 600	40	50	6
1:1 SDP3S/betaine	> 600	45	55	6
betaine	> 600	55	135	9
SDP3S (prespread oil layer)	55	35	—	50–80
1:1 SDP3S/betaine (pre-spread oil layer)	1500	28	—	45
betaine (pre-spread oil layer)	120	40	—	20
SDP3S (coarse emulsion)	75	40	35	13
1:1 SDP3S/betaine (coarse emulsion)	280	30	100	12
betaine (coarse emulsion)	300	50	50	10

boosting effect of betaine in the absence of antifoam is the increased foamability (higher initial foam volume).

### 3.3.2.2. Experiments with Pre-Spread Layer of Silicone

**Oil.** These experiments are aimed at comparing the stability of foam films in the presence of a spread oil layer. The observations show that the film thickness is not uniform in these experiments—the spread layer forms patches of irregular shape on the film surfaces. For that reason the values of the film thickness presented in Table 2 are estimated from the average intensity of the light reflected by the film at the moment of its rupture. Note that the quoted film thickness includes the thickness of the spread oil layer, i.e., the thickness of the aqueous core of the film is smaller.

In general, the foam films formed through a pre-spread layer of oil live shorter and typically rupture during the process of black film expansion (that is why there are no values for  $\tau_E$  in Table 2). Notably, films obtained from mixed surfactant solution live much longer (20–30 min) than films from SDP3S (1 min) and betaine (2 min).

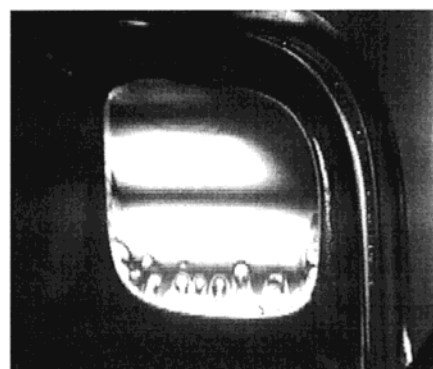
**3.3.2.3. Spreading of Oil During the Process of Film Drainage.** These experiments mimic to some extent the process in which an oil drop enters the solution surface at the PB and creates a source of spreading oil. In all cases the spreading of oil results in a significant disturbance of the film thinning pattern—the interference stripes become irregular and for several seconds move upward, which indicates an actual increase of the film thickness due to the Marangoni effect (the spreading oil drags liquid into the foam film).<sup>40</sup> The spreading oil induces film rupture in all systems, but the delay is different for the various solutions. The films obtained from betaine solutions rupture almost immediately after oil spreading, whereas the films from SDP3S solutions rupture about 10 s later. The films obtained from mixed surfactant solution are most resistant and live more than a minute after oil spreading.

The comparison with the previous experiments (pre-spread oil layer) shows that the dynamic process of spreading is much more dangerous for the foam films than the presence of a pre-spread layer. As discussed below, the entry of an oil drop at the surface of the PB leads to an oil spreading with subsequent perturbation and rupture of the neighboring foam films.

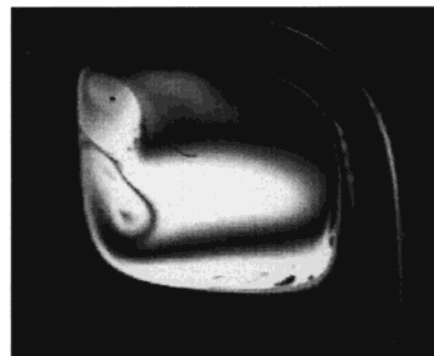
**3.3.2.4. Experiments with Surfactant Solutions Containing Emulsified Silicone Oil.** These experiments are performed with the coarse emulsion, which is used in the foam stability experiments as well (Ross–Miles test). The three-legs frame,<sup>31</sup> which ensures the formation of PB between three foam films, is employed.

A general feature in these experiments is that the thinning pattern of the first three films, formed from the working solutions (containing oil drops), is initially identical to that for films in the absence of oil—the interference stripes are horizontal and very regular, and the drainage time is similar to that in the absence of oil. However, a disturbance in the interference pattern of the thinning film is suddenly observed. The shape of the interference stripes becomes irregular, thus indicating a spreading of oil on the film surfaces, and soon after that the film ruptures—see Figure 9. A closer inspection of the Plateau borders by high-magnification optical lens shows that the PBs are crowded with oil droplets. Therefore, the observed change in the interference pattern can be interpreted as an oil drop entry in the region of the PB, which leads to fast oil spreading and film rupture.

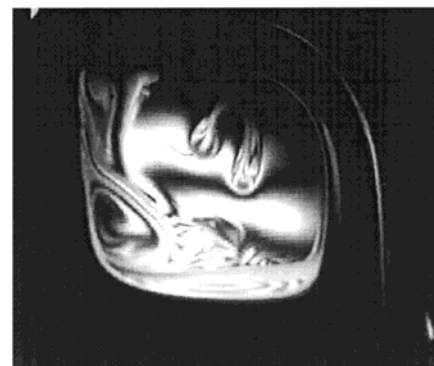
The accumulation of oil drops in the PB was directly observed in experiments with both vertical films and real foams, see Figures 10 and 11. In reflected light one can



(A)



(B)



(C)

**Figure 9.** Vertical foam films obtained from 0.1 wt % emulsion of silicone oil in 0.1 M SDP3S solution. The three-legs frame is used: (A) regular drainage of the vertical film; (B) an oil drop enters in the region of the PB and causes hydrodynamic instability in the film; (C) further development of the instability—the film ruptures several seconds later. Only one of the three films hung on the three-legs frame is seen bright in reflected light; the Plateau border formed between these three films is situated on the left-hand side of the bright film.

see a large number of oil droplets in the thick foam film, immediately after its formation from a silicone emulsion (Figure 10A). However, the oil drops are expelled out of the film almost instantaneously, because the film thickness becomes smaller than the drop diameter (Figure 10B)—no drop entry or film rupture are observed at that moment. The oil drops are sorted out and trapped in the narrowing PB with the further process of liquid drainage (Figure 10C). At a later stage, a drop entry with subsequent film rupture occurs, when the PB cross section becomes smaller than the drop diameter, and the compressing pressure exceeds the disjoining pressure barrier in the asymmetric oil–water–air film (Figure 9).

(40) Raczy, G.; Koczko, K.; Wasan, D. T. *J. Colloid Interface Sci.* **1996**, *181*, 124.

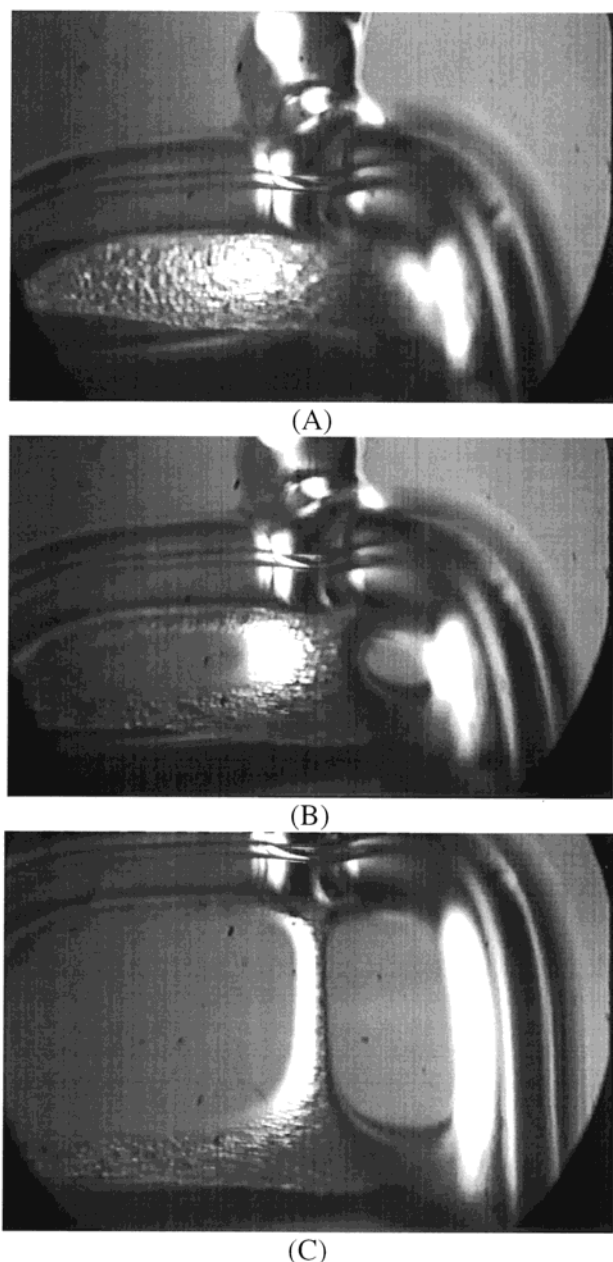


**Figure 10.** Three consecutive stages of foam film formation in the presence of silicone oil drops: (A) many oil drops are seen in the film area just after film formation; (B) the oil droplets leave the film and enter the Plateau border; (C) the oil drops are captured in the narrowing Plateau border. The vertical films are formed on the three-legs frame.

Numerous oil drops are seen in the PBs of the real foam—see Figure 11. The droplets in Figure 11 are strongly compressed within the narrow PBs, which is evidenced by the wavy contour of the border (induced by the entrapped droplets). Notably, the droplet concentration in the PBs is very high—the droplets form long, closely packed trains along the PBs, which certainly obstruct the borders and suppress the liquid drainage from the foam. For comparison, the average concentration of oil in the working solutions is only 0.1 vol. %. The accumulation of oil drops in the foam is caused by two main processes: first, the oil drops float up due to gravity (the mass density of the oil is  $0.93 \text{ g/cm}^3$ ) and second, the drops are trapped in the narrowing PBs of the foam and cannot follow the draining water. There is a substantial accumulation of oil in the foam as a result of these processes, which contributes to the overall destabilization of the system.

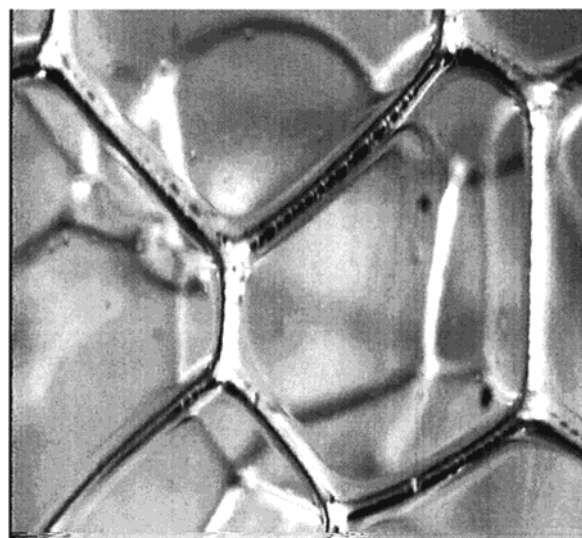


**Figure 11.** Photograph of foam cells in a real foam—many oil drops are seen trapped in the Plateau borders (0.1 M SDP3S, 0.1 wt % silicone oil, coarse emulsion).

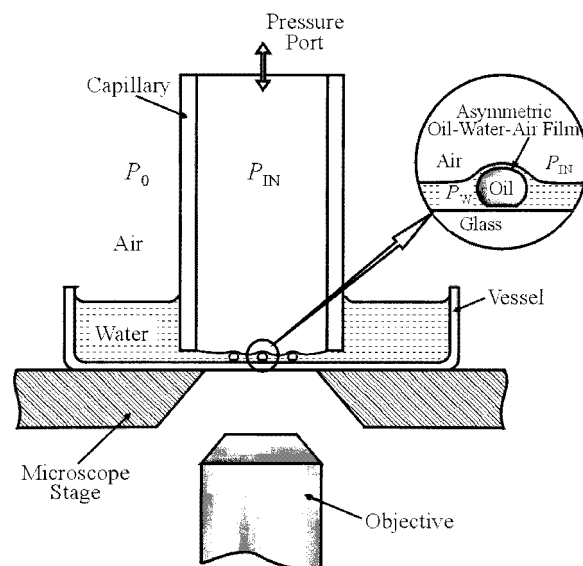


**Figure 12.** Scheme of the experimental setup for FTT experiments.

**3.4. Critical Capillary Pressure for Drop Entry Measured by Film Trapping Technique (FTT).** Recently Hadjiiski et al.<sup>41</sup> succeeded in measuring directly the critical capillary pressure leading to rupture of the asymmetric oil–water–air film (and to subsequent oil drop entry) by using a new version of the so-called Film Trapping Technique.<sup>42</sup> A schematic presentation of the principle of FTT is shown in Figure 12. A vertical capillary, partially filled with working solution, is placed in a close vicinity above the glass substrate. The capillary is connected to a pressure control system, which allows one to vary and to measure the difference,  $\Delta P$ , between the air pressure in the capillary,  $P_{IN}$ , and the ambient atmospheric pressure,  $P_0$ , with an accuracy of  $\pm 20 \text{ Pa}$ . When the air pressure  $P_{IN}$  increases, the air–water meniscus in the capillary is pushed against the glass substrate—a wetting film is formed, which traps some of

(41) Hadjiiski, A.; Cholakova, S.; Ivanov, I. B.; Gurkov, T. D.; Leonard, E. *Langmuir*, submitted.

(42) Hadjiiski, A.; Dimova, R.; Denkov, N. D.; Ivanov, I. B.; Borwankar, R. *Langmuir* **1996**, *12*, 6665.



the oil droplets dispersed in the working solution. These drops remain sandwiched between the water–air and glass–water interfaces. The droplets are observed from below, through the glass substrate, by means of an inverted optical microscope. Upon further increase of the capillary pressure,  $\Delta P = (P_{\text{IN}} - P_0)$ , some of the trapped drops enter the air–water interface. Therefore, the equipment allows one to measure the critical capillary pressure for drop entry,  $\Delta P_{\text{CR}}$ , as a function of the solution composition and drop radius. A larger pressure difference,  $\Delta P_{\text{CR}}$ , corresponds to a higher barrier (more difficult drop entry) and vice versa. More technical details about the FTT, and a wider description of its application to various systems, can be found in the methodological papers.<sup>41,42</sup>

Mixtures of SDP3S and betaine at four different molar ratios (100:0, 80:20, 70:30, 0:100) are studied by FTT. The results show that: (1) there is a big difference between the values of the critical pressure,  $\Delta P_{\text{CR}}$ , for different surfactant compositions; and (2) there is a trend of decreasing  $\Delta P_{\text{CR}}$  with drop size. The critical pressure,  $\Delta P_{\text{CR}}$ , is about 180 Pa for solutions of SDP3S (no booster) at a drop diameter of about 11  $\mu\text{m}$ , which is the average drop size in the coarse emulsion used in the foam tests (for comparison,  $\Delta P_{\text{CR}} \approx 400$  Pa for a drop size of 6  $\mu\text{m}$ , which is the mean drop size in the fine emulsion). The critical pressure is  $\Delta P_{\text{CR}} \approx 850$  Pa for a drop size of 11  $\mu\text{m}$  in the of system SDP3S/betaine = 80:20, and it is slightly higher at a molar ratio of 70:30 (900 Pa). The experiments with a solution of betaine (no SDP3S) show that  $\Delta P_{\text{CR}}$  is very high and exceeds the working range of the experimental system (above 7000 Pa). Note that the observed increase of the critical capillary pressure with betaine concentration correlates very well with the observed trends in the foam stability tests.

#### 4. Discussion

**4.1. Mechanism of Foam Destruction by Oil Droplets.** The brief literature overview presented in Section 1 shows that an uncertainty still exists about the actual mechanisms of foam destruction by oil-containing anti-foams. Except for a few studies, the interpretation of the experimental results in the literature is made at a level of hypotheses, which cannot be verified by the available experimental information. The combination of several complementary methods for observation of the processes in foams and foam films provides a deeper insight into the antifoaming effect of oil in the studied systems.

The experiments with foam films show that the oil droplets are not able to overcome the barrier to particle entry unless they are strongly compressed against the air–water interface (the possible origin of the entry barrier is discussed at the end of Section 4.2). As a result of this high barrier, the droplets are expelled from the films into the neighboring PBs during the stage of film thinning. Indeed, the capillary pressure,  $\Delta P_{\text{F}}$ , which compresses the droplets in the thinning films is of the order of the capillary pressure created by the curved meniscus surrounding the film; for wet foams  $\Delta P_{\text{F}}$  can be estimated from the Laplace equation

$$\Delta P_{\text{F}} = 2\sigma_{\text{AW}}/R_{\text{B}} \quad (4)$$

where  $R_{\text{B}}$  is the radius of the foam bubbles. Introducing typical values in eq 4,  $\sigma_{\text{AW}} \approx 25$  mN/m and  $R_{\text{B}} \approx 1$  mm, one obtains  $\Delta P_{\text{F}} \approx 50$  Pa, which is well below the barrier measured by FTT (between 180 and 400 Pa). One can conclude that the droplets are pushed away by the approaching surfaces of the thinning films. Note that the entry coefficient of all studied systems is strongly positive,

which means that the entry process is thermodynamically favorable, but cannot be realized at the stage of film thinning, because the drops do not have enough energy to overcome the barrier.

Much higher capillary pressures are realized in the Plateau borders as the liquid drains from the foam. The net driving forces for film and PB border drainage must be zero at mechanical equilibrium. This means that for both types of films, symmetrical foam films and asymmetric oil–water–air films, the disjoining pressure must counterbalance the suction (capillary) pressure in the Plateau border, which is created by the curvature of the air–water wall of the PB. On the other hand, the condition for mechanical equilibrium in the foam column requires the appearance of a suction pressure gradient which opposes gravity.<sup>43</sup> In equilibrium one can estimate the magnitude of the suction capillary pressure,  $P_{\text{C}}(H)$ , at a given level of the foam column from the height,  $H$ , of this layer above the level of the bulk liquid<sup>43</sup>

$$P_{\text{C}}(H) = \frac{1}{2}\Delta P_{\text{F}} + P_{\text{HYDR}} = \frac{\sigma_{\text{AW}}}{R_{\text{B}}} + \Delta\rho gH \quad (5)$$

Here  $\Delta\rho = 1000$  kg/m<sup>3</sup> is the difference between the mass densities of the aqueous and the gaseous phases and  $g = 9.8$  m/s<sup>2</sup> is the acceleration of gravity. Equation 5 shows that the capillary pressure increases with the height of the foam column. Let us estimate  $P_{\text{C}}$  for the upper layer in the final (static) foams obtained from SDP3S/betaine solutions (80:20) in the presence of silicone oil. The final height of the foam column measured in the experiments with this system is equal to  $H = 10.7$  cm ( $H$  can be calculated from the final foam volume and the diameter of the cylinder in the Ross–Miles test), which corresponds to hydrostatic pressure  $\Delta P_{\text{HYDR}} = \Delta\rho gH \approx 1040$  Pa, and to capillary pressure  $P_{\text{C}} \approx 1065$  Pa. These values are comparable in magnitude to the barrier measured by FTT,  $\Delta P_{\text{CR}} \approx 850$  Pa. Similarly, for foams produced from SDP3S (no betaine) one can estimate  $H = 4.6$  cm,  $\Delta P_{\text{HYDR}} \approx 450$  Pa, and  $P_{\text{C}} \approx 475$  Pa, which is also on the same order of magnitude as the measured entry barrier by FTT,  $\Delta P_{\text{CR}} \approx 200$  Pa.

We should emphasize that the magnitudes of the critical pressure,  $\Delta P_{\text{CR}}$ , measured by FTT, and the capillary suction pressure in the foam column,  $P_{\text{C}}$  (eq 5), should not necessarily be equal to each other—only the general trends of their variation upon changing a given parameter (e.g., the surfactant composition or the oil drop size) are expected to be similar. The reason is that  $\Delta P_{\text{CR}}$  and  $P_{\text{C}}$  are both unequal to the height of the disjoining pressure barrier,  $\Pi_{\text{MAX}}$ , which is the actual factor opposing the rupture of the asymmetric film (Figure 13). Since the oil drops in the PBs and in the wetting films (in FTT) are relatively small, there are significant capillary pressure jumps across the curved oil–water interface and the asymmetric films; these capillary pressures also contribute to the general pressure balance in the system. That is why one cannot directly equalize  $\Pi_{\text{MAX}}$  to  $\Delta P_{\text{CR}}$  or to  $P_{\text{C}}$ . A further mechanical model of the process of drop entry in the PBs and in FTT experiments has to be developed for calculating the value of  $\Pi_{\text{MAX}}$  from the experimental data.

The agreement between the observed trends (and orders of magnitude) of  $P_{\text{C}}$  and  $\Delta P_{\text{CR}}$  with the variation of betaine concentration suggests the following interpretation of the

(43) Narsimhan, G.; Ruckenstein, E. In *Foams: Theory, Measurements, and Applications*; Prud'homme, R. K., Khan, S. A., Eds.; Surfactant Science Series; Marcel Dekker: New York, 1996; Vol. 57, Chapter 2.

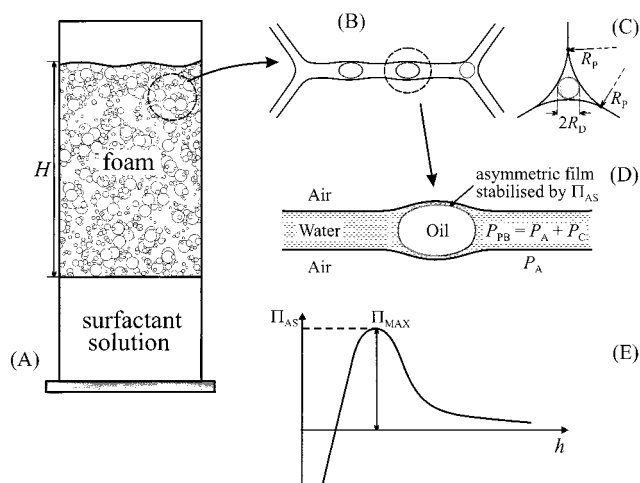


**Figure 13.** Schematic presentation of the mechanism of foam destruction by oil drops: (A, B) the oil drops are rapidly expelled from the foam films into the Plateau borders, where they are strongly compressed (D) by the walls of the narrowing PB—symmetric oil–water–air films, formed between the drops and the walls of the PB. When the sucking capillary pressure in the PB becomes high enough, the disjoining pressure barrier stabilizing the asymmetric film,  $\Pi_{\text{MAX}}$ , is overcome (E) and the asymmetric film ruptures. The subsequent drop entry leads to oil spreading, mechanical shock on the neighboring foam films and eventually, to their rupture. The radius of curvature of the PB walls,  $R_p$ , and the radius of a drop,  $R_D$ , which fits the cross-section of the PB are schematically shown in (C).

experimental data about the final foam volume in these two systems (SDP3S and 80:20 SDP3S/betaine). The capillary pressure is low just after foam formation, and the oil droplets are expelled from the films into the Plateau borders without entry and foam film rupture. As the liquid drains from the foam, the capillary pressure in the upper part of the foam column gradually increases up to values that are comparable to the barrier opposing the drop entry. This leads to strong compression of the droplets (Figure 11) and when the capillary suction pressure,  $P_C$ , becomes large enough, the disjoining pressure barrier,  $\Pi_{\text{MAX}}$ , stabilizing the asymmetric film is overcome—the oil drops are forced to enter the surface (Figure 13). As demonstrated in Figure 9, such an entry leads to subsequent film rupture. According to this picture, the foam will decay until the capillary pressure,  $P_C$ , at the top of the foam column becomes comparable to the entry barrier.

The above consideration can be developed further to explain the enhanced stability of foams in the presence of *smaller* droplets of silicone oil (fine emulsion). As mentioned in Section 3.4 above, the entry barrier increases for smaller droplets. One additional requirement for realization of the mechanism described above is that the cross section of the PB should be smaller than the drop diameter (otherwise, the drops are not compressed by the walls of the PB). Therefore, the water drainage has to evolve longer until narrower Plateau channels are obtained in the case of smaller oil droplets. Moreover, the equilibrium cross section of the channels may be larger than the drop diameter in the entire foam column. The droplets are unable to break the foam in this case even after a very long time, because they are not compressed by the air–water interfaces (no drop entry occurs). As a consequence, the oil drops do not exhibit any antifoam action. The radius of the sphere that fits the cross section of the PB can be estimated from the equation

$$R_D = \left( \frac{2\sqrt{3}}{3} - 1 \right) R_p \approx 0.155 R_p \quad (6)$$

where

$$R_p = \frac{\sigma_{\text{AW}}}{P_C} \quad (7)$$

is the radius of curvature of the air–water interface at the PB (Figure 13). Equation 6 is obtained by assuming that the contact angle foam film meniscus is equal to zero; positive values of the contact angle correspond to a narrower Plateau channel, i.e., to a smaller  $R_p$ . Introducing the values for a SDP3S solution in eqs 6 and 7, we obtain  $R_p \approx 50 \mu\text{m}$  and  $R_D \approx 8 \mu\text{m}$ . These results mean that if the silicone oil drops are smaller in radius than  $R_D$ , (cf. the drop size in the coarse and fine emulsions), then the final static foam column would be higher than the value predicted by the entry barrier. In such a case, the static height of the foam column would depend on both the entry barrier and the drop size (this is the case in foam experiments with the fine emulsion). On the contrary, if the drop radius is larger than  $R_D$ , then the static height of the foam column is determined primarily by the entry barrier (foam experiments with the coarse emulsion).

The explanations described above oversimplify to some extent the real situation, because they neglect several effects that might be important in some systems. For instance, two such effects are: (1) the presence of droplets that have much larger size than the average one in polydisperse emulsions, and (2) the possibility for accumulation of many oil drops in a given PB, where a process of drop coalescence might take place, thus increasing the actual average drop size. The contribution of these two effects can be evaluated only after developing a detailed mechanical model of the drop entry event which accounts for the drop size and shape, and considers quantitatively the stability of the asymmetric (oil–water–air) and emulsion (oil–water–oil) films.

We have to admit that the final step of PB destruction in the studied systems still remains unclear. It might be any of the mechanisms discussed in the literature—bridging-stretching, bridging-dewetting, or spreading-fluid entrainment. Moreover, the entry of a strongly compressed droplet in the PB certainly creates a strong mechanical shock on the neighboring foam films. The instant release of surface energy, accumulated during the process of drop compression and deformation, probably resembles a small explosion which is able to destroy the neighboring thin foam films as a result of the propagating mechanical stress. For brevity, hereafter we call this mechanism of foam destruction the bursting mechanism (or compression-bursting if we follow the tradition in the antifoam literature to identify the consecutive stages of the process). It is worth noting that this mechanism is a manifestation of a more general type of phenomenon, usually termed in the scientific literature catastrophe or bifurcation.<sup>44</sup> A common feature of these phenomena is that some type of instability (the instability of the asymmetric film in our system) appears in the moment when a smoothly varying parameter (the capillary pressure,  $P_C$ , in our case) exceeds a certain critical value.<sup>44</sup> One possible way to reveal further details in the critical step of foam destruction might be the optical observation

(44) Thompson, J. M. T. *Instabilities and Catastrophes in Science and Engineering*; John Wiley & Sons: New York, 1982.

of the process of PB destruction using a high-speed camera.<sup>21,45</sup>

At the end of this section we would like to compare briefly the mechanism of antifoam action observed in the present study with the results from ref 21. The main difference of the experimental system in ref 21 is that the antifoam globules contained hydrophobic solid silica particles. As discussed by Garrett,<sup>11</sup> Bergeron et al.,<sup>10</sup> and Aveyard and Clint,<sup>46</sup> the solid silica particles greatly reduce the barrier to entry of the antifoam globules. As a result, the antifoam globules are able to enter the air–water interface and to make unstable bridges at the early stages of foam film thinning (these events were directly observed by high speed videocamera in ref 21). In other words, the antifoam droplets containing silica are very active, and they are able to destroy the thinning foam films within several seconds, which leads to very rapid destruction of the overall foam (ca. within 5–10 s). However, if the antifoam globules are unable to destroy the foam films (for example, in an already exhausted antifoam<sup>40,47</sup>), then the antifoam globules are expelled into the neighboring PBs, and a much longer time is necessary for foam destruction to occur—typically tens of minutes (just as in the present study).

#### 4.2. Mechanism of Foam Stabilization by Betaine.

As discussed in Section 3.1, the foam produced from SDP3S solutions (no betaine) is stable in the absence of silicone oil. Therefore the boosting effect of betaine *in the absence* of oil can be explained by the larger *initial volume* of the produced foam at comparable conditions. Indeed, the introduction of betaine to SDP3S solutions (at fixed total concentration of surfactants) leads to a notable increase of the initial foam volume. This effect is well-known in the literature and might be explained by reduced dynamic surface tension of the mixed surfactant solutions. A lower dynamic surface tension would lead to easier expansion of the solution surface, and hence, to better foamability of the solutions.

The boosting effect of betaine *in the presence* of silicone oil is a much more complex and less understood phenomenon. From the literature overview (Section 1) one can deduce, in principle, two qualitatively different explanations of the boosting effect. One possibility is that the booster changes the interfacial tensions with subsequent reduction of the values of  $E$ ,  $S$ , and/or  $B$  coefficients. Such a reduction of the coefficients would make more unfavorable the processes of entry, spreading, and/or bridge rupture in the presence of oil. As a result, the foam would become more stable. Another possibility is that the booster stabilizes the asymmetric oil–water–air film, thus preventing the entry of the droplets. In this case the processes of entry, spreading, and bridge rupture might still be thermodynamically favorable, but strongly suppressed by the enhanced stability of the asymmetric films.

The results presented in Sections 3.2–3.4 unambiguously show that *the main role of betaine in the studied systems is to increase the barrier to drop entry*. Indeed,  $E$ ,  $S$ , and  $B$  coefficients are positive for all systems, and no correlation between their values and the foam stability is observed. Additionally, measurements of the critical capillary pressure inducing drop entry (Section 3.4) have shown that the critical pressure strongly increases in the presence of betaine.

An interesting question is, what is the detailed molecular mechanism leading to the higher entry barrier in the presence of betaine. One may expect that the introduction of betaine into the surfactant solution leads to denser adsorption layers, but it is not obvious how exactly this change would enhance the stability of the asymmetric oil–water–air film. This point deserves further investigation by determining the surfactant adsorption on the air–water and oil–water interfaces in mixed systems, and by analyzing the different components of the disjoining pressure in the asymmetric film. In principle, the entry barrier in the system under consideration might be due to electrostatic repulsion, van der Waals repulsion, and/or micelle structure forces. To analyze in detail the effect of betaine on the entry barrier, one should dispose of information about the electrical surface potential at the oil–water and air–water interfaces, as well as about the properties of the mixed micelles (aggregation number, size, charge). Such a detailed study of the molecular mechanism of the boosting effect is currently underway.

### 5. Conclusions

A set of complementary experiments is performed with foams and foam films stabilized by a mixture of two surfactants: an anionic surfactant (SDP3S) as the main stabilizing agent, and an amphoteric surfactant (betaine) as the foam booster. The main goal of the study is to clarify: (1) the mechanism of foam destruction by droplets of silicone oil, and (2) the factors responsible for the foam boosting effect of betaine in the presence of oil. The conclusions from the obtained results can be summarized in the following way:

(i) Experiments using the Ross–Miles test demonstrate that the foams are stable for all surfactant compositions *in the absence of silicone oil*. The boosting effect of betaine in these systems is manifested as a higher foamability of solutions containing surfactant mixtures.

(ii) Foam stability experiments *in the presence of oil* show that foams containing SDP3S alone (or betaine of low relative concentration) are unstable and decay with time. The foam stability increases with the relative concentration of betaine if the anionic surfactant (SDP3S) is in excess. Above a certain relative concentration of betaine (around 40 molar %) the foams are stable and do not decay within the experimental timescale (100 min). One important conclusion from a practical viewpoint is that the *size of the emulsion droplets* has a significant effect on the foam stability. One can introduce a substantial amount of silicone oil in the surfactant solution without deteriorating the foam stability, if the oil droplets have a diameter of ca. 5  $\mu\text{m}$  and below.

(iii) Direct observations of the thinning of foam films in the presence of oil droplets show that these droplets leave the films relatively rapidly (typically, for less than a minute) without destroying them. The foam destruction occurs when the oil droplets are compressed by the walls of the narrowing Plateau channels in the process of liquid drainage from the foam.

(iv) Surface and interfacial tension measurements show that entry,  $E$ , spreading,  $S$ , and bridging,  $B$ , coefficients are all positive. Thus the classical approach to antifoaming, which does not account for the entry barrier of oil drops, predicts a very high efficiency of the silicone oil as an antifoam in all these systems (which is not observed in the Ross–Miles test). There is no correlation between the values of  $E$ ,  $S$ , and  $B$  on one side, and the foam stability on the other side. Therefore, the variations in the values of  $E$ ,  $S$ , and  $B$  coefficients cannot be used to explain the observed trends in foam stability.

(45) Dippenaar, A. *Int. J. Mineral. Process.* **1982**, 9, 1.

(46) Aveyard, R.; Clint, J. H. *J. Chem. Soc., Faraday Trans.* **1995**, 91, 2681.

(47) Denkov, N. D.; Marinova, K.; Christova, C.; Hadjiiski, A.; Cooper, P. *Langmuir*, submitted.



The critical capillary pressure inducing drop entry (and hence, the entry barrier) increases strongly with the relative concentration of betaine. The results imply that the foam destruction in the studied systems occurs through a catastrophic<sup>44</sup> type of process—when the smoothly increasing capillary pressure at the top of the foam column exceeds a given critical value (which is related to the magnitude of the entry barrier), the drops are forced to enter the surface of the PB. The drop entry leads to oil spreading, mechanical disturbance of the neighboring foam films, and film rupture. One can conclude that the main role of betaine as a booster in the studied systems is to increase the barrier to drop entry. Furthermore, foam films obtained from mixed surfactant solutions (1:1 SDP3S/betaine) are more stable and live longer in the

presence of a spread oil layer compared to films stabilized by the individual surfactants.

A further systematic study is underway to develop a mechanical model of the drop entry event in the Plateau borders, and to reveal the molecular explanation of the increased entry barriers in the presence of betaine.

**Acknowledgment.** The support of this study by Kao Co., Japan, is gratefully acknowledged. The authors are indebted to Dr. A. Hadjiiski and Mrs. S. Cholakova for providing the results obtained by FTT prior to publication, to Mrs. M. Temelska for the foam stability tests, as well as to Prof. I. B. Ivanov, Prof. P. A. Kralchevsky, and Dr. S. Stoyanov for helpful discussions.

LA990777+